

# High-Pressure Behavior of Lead Cyanamide PbNCN

Andreas Möller,<sup>[a]</sup> Philipp M. Konze,<sup>[a]</sup> and Richard Dronskowski\*<sup>[a,b]</sup>

*Dedicated to Professor Wolfgang Bensch on the Occasion of his 65th Birthday*

**Abstract.** The high-pressure behavior of lead cyanamide, PbNCN, was studied using the diamond anvil cell technique and in situ X-ray powder diffraction at room temperature. By employing a third-order Birch–Murnaghan equation of state, a zero-pressure bulk modulus of  $K_0 = 19(2)$  GPa was determined, characterizing PbNCN as a very soft material. Additionally, the first linear compression moduli for the inorganic cyanamide were determined to be  $K_{a0} = 145(7)$  GPa,  $K_{b0} =$

$37.7(7)$  GPa, and  $K_{c0} = 15.5(2)$  GPa. DFT total-energy calculations targeting on the  $\text{Pb}^{2+}$  coordination indicate a transition from a typical compression behavior of a two-dimensional layered structure to a more complex one, which was furthermore analyzed by chemical-bonding analysis. Instead of a changing shape of the soft cyanamide unit, we observe an unexpected flattening of the corrugated double layers.

## Introduction

Deprotonated  $\text{H}_2\text{NCN}$ , found both in its asymmetric  $\text{N}=\text{C}\equiv\text{N}^{2-}$  cyanamide and symmetric  $\text{N}=\text{C}=\text{N}^{2-}$  carbodiimide form, has been known since the discovery of  $\text{CaNCN}$  in 1895.<sup>[1]</sup> More recently the class of solid-state carbodiimides and cyanamides has grown significantly with the synthesis of binary and ternary alkali,<sup>[2]</sup> alkaline-earth,<sup>[3]</sup> main-group,<sup>[4]</sup> transition,<sup>[5]</sup> and rare-earth<sup>[6]</sup> metal phases. Especially transition-metal carbodiimides exhibit a variety of interesting physical properties, often with enhanced functionality over their oxide analogues, for example as heterogeneous non-oxidic water-oxidation catalysts.<sup>[7]</sup> Recently it has been shown that  $\text{MNCN}$  ( $M = \text{Mn} - \text{Zn}$ ) and also  $\text{Cr}_2(\text{NCN})_3$  are electrochemically active in Li and Na batteries.<sup>[8]</sup>

Over the past three decades, metal cyanamides have been systematically studied at ambient conditions, but their high-pressure behavior remained almost unexplored. A single exception is made by mercury cyanamide,  $\text{HgNCN}$ ,<sup>[9]</sup> which undergoes a simple decomposition at 1.9 GPa. Nonetheless, the high-pressure behavior of other, more stable, heavy metal cyanamides could provide a more elaborate insight into the high-pressure behavior of carbodiimides and cyanamides.

In this work, we present the high-pressure behavior of PbNCN by determining unexpected structural changes and bulk moduli up to 6.5 GPa. We support these findings with density-functional theory calculations on the behavior of the lead coordination up to 13 GPa. The results are carefully analyzed by means of chemical-bonding analysis.

\* Prof. Dr. R. Dronskowski  
E-Mail: drons@HAL9000.ac.rwth-aachen.de

[a] Chair of Solid State and Quantum Chemistry  
Institute of Inorganic Chemistry  
RWTH Aachen University  
52056 Aachen, Germany

[b] Jülich-Aachen Research Alliance (JARA-HPC and JARA-FIT)  
RWTH Aachen University  
52056 Aachen, Germany

## Experimental Section

**Methods:** Powderous lead cyanamide was prepared following the procedure by Liu et al.<sup>[10]</sup> Lead acetate ( $0.1 \text{ mmol}\cdot\text{L}^{-1}$ ) and cyanamide ( $0.1 \text{ mmol}\cdot\text{L}^{-1}$ ) were mixed as aqueous solutions followed by addition of diluted ammonia solution to reach a pH value of 10. The bulky yellow precipitate was filtered off, washed with water and dried in vacuo. The high-pressure measurements were carried out at room temperature in a Boehler-Almax diamond anvil cell (DAC) with  $400 \mu\text{m}$  cutlets. CuBe disks with predrilled  $150 \mu\text{m}$  sample chambers were used as gasket material. The powdered sample, a few ruby spheres, and a 4:1 mixture of methanol and ethanol – as the pressure-transmitting medium – were placed in the sample chamber. Set pressures were allowed to equilibrate for 1 h before being measured by the ruby fluorescence method.<sup>[11]</sup> The pressure was re-determined after each collected diffraction pattern to ensure static pressures with an uncertainty of less than 0.02 GPa. Diffraction patterns were collected with a Stoe StadiMP (Mo- $K_{\alpha 1}$ ,  $\lambda = 0.709319 \text{ \AA}$ ) equipped with a Dectris Mythen-detector between  $7\text{--}24$ ; in  $2\theta$ . Lattice parameters were obtained through full profile refinement using the LeBail method, as implemented in the FullProf suite.

**Computational Details:** All calculations were based on density-functional theory (DFT) using the PBE functional<sup>[12]</sup> and adding the many-body-dispersion (MBD) correction scheme to account for the lack of dispersion interactions in DFT.<sup>[13]</sup> Plane-wave basis sets and the projector augmented wave (PAW) method<sup>[14]</sup> was used as implemented in the Vienna Ab initio Simulation Package (VASP).<sup>[15]</sup> We also included the Pb 5d semi-core levels in all calculations and chose an energy cutoff for the plane-wave expansion of 600 eV. The electronic convergence criterion was set to  $10^{-7}$  eV, while structural optimization was performed until residual forces fell below  $5 \times 10^{-3} \text{ eV}\cdot\text{\AA}^{-1}$ . Reciprocal space was sampled on  $\Gamma$ -centered  $k$ -point grids with densities of  $0.02 \text{ \AA}^{-1}$ . Chemical-bonding analyses of plane-wave data was performed using LOBSTER,<sup>[16]</sup> which allows us to project plane-wave data to an atomic basis to generate Crystal Orbital Hamilton Population (COHP)<sup>[16a]</sup> plots.

## Results and Discussion

At ambient conditions, lead cyanamide, PbNCN, crystallizes in the orthorhombic space group  $Pnma$  with lattice parameters

of  $a = 5.5566(4)$  Å,  $b = 3.8677(2)$  Å, and  $c = 11.7350(8)$  Å (see Figure 1a).<sup>[17]</sup> The single-crystal X-ray structure determination corroborates PbNCN to adopt a linear cyanamide motif with C–N = 1.30(3) Å and C≡N = 1.16(3) Å, and it further shows that in the  $ab$  plane NCN<sup>2-</sup> and Pb<sup>2+</sup> form corrugated double layers, which are stacked along the  $c$  axis. The coordination sphere of lead is a distorted square pyramidal shape that is augmented by two second-nearest nitrogen atoms, so the coordination number (CN) equals 5 (+2). Hence, one finds one short Pb–N(1) bond of 2.31(2) Å almost parallel to the  $c$  axis, plus two Pb–N(1) and two Pb–N(2) bonds of 2.62(1) Å length each. The distance of the second-nearest neighbors Pb···N(2) = 3.43(1) Å is to be classified as non-binding<sup>[17]</sup> and corresponds to the distance of the corrugated layers (Figure 1b, dashed bonds). Indeed, the first five Pb–N bonds are sufficient to arrive at an empirical bond-valence sum of 2.14 for Pb<sup>2+</sup>, as shown earlier.<sup>[17]</sup>

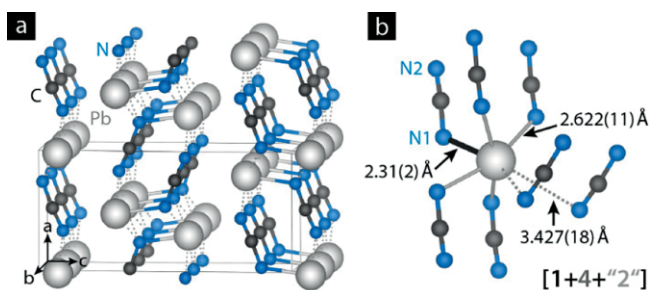


**Figure 1.** (a) Crystal structure of PbNCN and (b) perspective view of Pb coordination with dashed bonds representing the nearest contact towards the neighboring double layer.

To investigate the high-pressure behavior of PbNCN, diffractograms up to a pressure of 6.49(1) GPa were recorded in a diamond anvil cell. The lattice parameters and cell volume as a function of pressure are shown in Figure 2a and b, respectively. Numerical values are given in Table 1. To determine the compression modulus, a third order Birch–Murnaghan equation of state in the form of an  $F$ - $f$  plot was used (Figure 2c). The linear regression arrives at a compression modulus of  $K_0 = 19(2)$  GPa with a first derivative of  $K' = 14(3)$ . This makes PbNCN a very soft material.

Since PbNCN has an orthorhombic unit cell containing the complex anion NCN<sup>2-</sup>, an anisotropic compression behavior may be expected. Figure 2d reveals that the lattice parameter  $a$  has the smallest change of 1.1 %, the  $c$  parameter the largest change of 9.4 %, and the change of the  $b$  parameter of 4.1 % is between these two. For rectangular crystal systems, the compression moduli of the individual lattice parameters can be determined by matching the same type of equation of state as the volume.<sup>[18]</sup> For the  $a$  axis, the fitting provides a compression modulus of  $K_{a0} = 145(7)$  GPa with  $K_{a'} = 44(7)$ , for the  $b$  axis of  $K_{b0} = 37.7(7)$  GPa with  $K_{b'} = 5.0(2)$ , and for the  $c$  axis of  $K_{c0} = 15.5(2)$  GPa with  $K_{c'} = 3.03(7)$ .

While the experimental results show a good fit using a single 3rd order Birch–Murnaghan equation, the cell volume, however, indicates a different kind of behavior around 3–4 GPa. Therefore, we employed DFT calculation up to 15 GPa

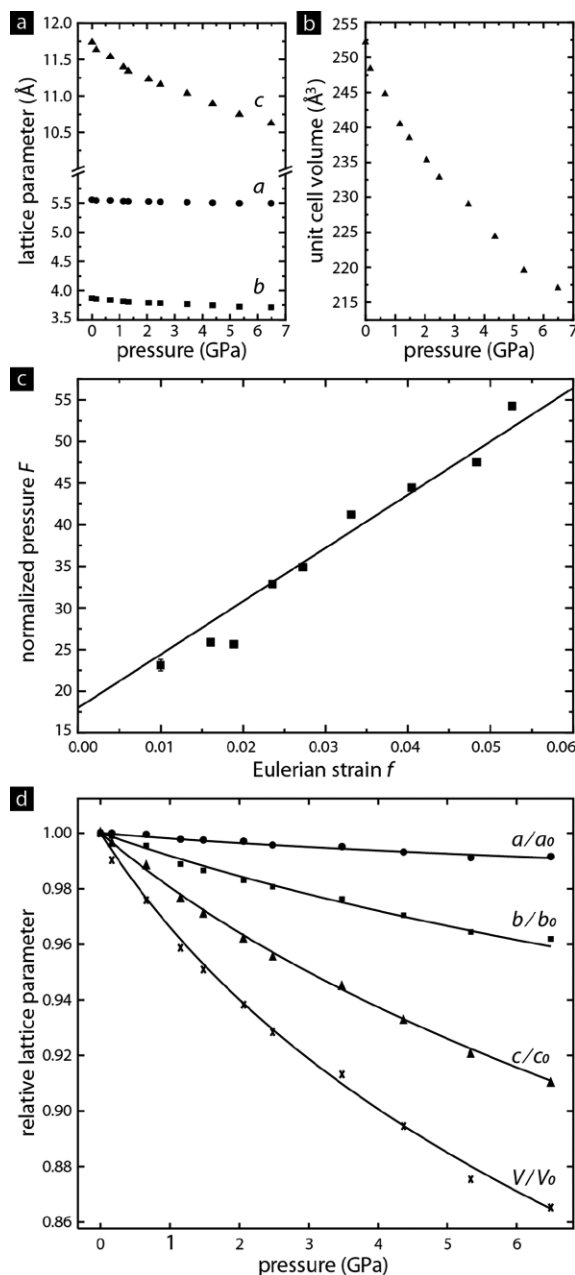


**Figure 2.** (a) Variation of lattice parameters and (b) volume of PbNCN with applied pressure. (c)  $F$ - $f$  plot and fit of a 3rd order Birch–Murnaghan equation of state. The intersection with the y axis shows the compression modulus  $K_0 = 19(2)$  GPa and the slope its first derivative  $K' = 14(3)$ . (d) Relative lattice parameters and cell volume with increasing pressure, including 3rd order Birch–Murnaghan fits. The size of the error bars lies within the size of the symbols. The error in pressure is smaller than 0.02 GPa.

to investigate the atomic positions, which are not available from experiment. Using the many-body dispersion correction<sup>[13]</sup> yields a very good agreement of the lattice parameters at ambient conditions (Table 2), and reproduces the Pb–N bonds reasonably well. We note that DFT is notoriously unreliable in correctly determining the energetics of the cyanamide/carbodiimide shape problem,<sup>[8,36]</sup> reflected in the less pro-

**Table 1.** Variation of lattice parameters and cell volume of PbNCN with pressure.

$p$ /GPa	$a$ /Å	$b$ /Å	$c$ /Å	$V$ /Å <sup>3</sup>
0.00	5.5566(4)	3.8677(2)	11.7350(8)	252.157(7)
0.16(2)	5.5430(5)	3.8514(2)	11.6353(1)	248.39(3)
0.66(2)	5.5412(8)	3.8379(5)	11.5376(21)	244.77(3)
1.15(2)	5.5321(5)	3.8133(4)	11.3990(10)	240.47(2)
1.48(2)	5.5299(12)	3.8041(6)	11.338(2)	238.50(4)
2.06(2)	5.5274(10)	3.7909(3)	11.2307(13)	235.33(4)
2.48(2)	5.5198(12)	3.7814(8)	11.156(4)	232.85(6)
3.61(2)	5.5173(5)	3.7649(3)	11.035(2)	229.04(3)
4.37(2)	5.5060(18)	3.7417(8)	10.891(4)	224.37(4)
5.34(2)	5.4950(2)	3.7184(1)	10.746(3)	219.57(6)
6.49(2)	5.4970(13)	3.7090(13)	10.627(5)	217.01(6)

**Table 2.** Theoretical structural parameters at 0, 5, and 13 GPa, as well as experimental results from single-crystal diffraction in reference<sup>[17]</sup>.

Parameter	Exp.	Calcd. 0 GPa	5 GPa	13 GPa
$a$ /Å	5.5566(4)	5.572	5.506	5.502
$b$ /Å	3.8677(2)	3.839	3.717	3.640
$c$ /Å	11.7350(8)	11.956	11.265	10.270
$V$ /Å <sup>3</sup>	252.2	255.7	230.5	205.7
$d(\text{Pb1-N1})$ /Å	2.31(2)	2.381	2.363	2.344
$d(\text{Pb1-N2})$ /Å	2.62(1)	2.658	2.546	2.506
$d(\text{Pb1-N2})^a$ /Å	3.43(1)	3.389	3.116	3.056
$d(\text{C1-N1})$ /Å	1.30(4)	1.248	1.243	1.245
$d(\text{C1-N2})$ /Å	1.16(3)	1.226	1.223	1.211
$d(\text{N1-N2})$ /Å	2.45(3)	2.473	2.464	2.456
Angle (N1-C1-N2) /°	176(3)	176.8	175.5	177.5
Angle ( $\vec{a}$ , N1-N2) <sup>b</sup> /°	22.5	24.9	24.6	14.2

a) Long bond, between neighboring corrugated double layers. b) Angle between the  $a$  lattice vector and  $\text{NCN}^{2-}$  unit, as indicated in Figure 3b.

nounced differences in C–N bond lengths. However, the overall size and shape of the cyanamide unit (N1–N2 distance and N1–C1–N2 angle, see Table 2) is in good agreement with experiments. Furthermore, we expect the difference in stiffness between cyanamide and carbodiimide units to be miniscule: For the two polymorphs of HgNCN the differences between the respective  $\delta$ ,  $\nu_{\text{S}}$ , and  $\nu_{\text{AS}}$  modes of  $\text{NCN}^{2-}$  are well below  $100 \text{ cm}^{-1}$ .<sup>[10,19]</sup>

When plotting the  $a$  lattice parameter and the unit cell volume from first-principles theory (Figure 3a), we observe a local minimum of  $a$  at around 5 GPa, followed by an increase up to 9 GPa. To investigate the reason for this behavior, we chose three cells at 0, 5, and 13 GPa. The resulting structures are shown in Figure 3b. Going from 0 to 5 GPa we compress the soft  $c$  axis, without significant changes in the double layers containing the [1+4] coordination. The longer Pb–N nonbonding contacts are compressed to 3.12 Å, which would lead to a sevenfold coordination of Pb. However, when compressing further to 13 GPa the two longer Pb–N bonds do not shorten but the tilted orientation of the  $\text{NCN}^{2-}$  unit begins turning towards the  $a$  axis. The overall shape of the  $\text{NCN}^{2-}$  anion remains largely unchanged during compression (Table 2). While the deformation mode of the cyanamide is soft,<sup>[17]</sup> the coordination in the case of PbNCN restricts its ability to bend during compression. Instead, we observe a flattening of the corrugated double layers. A similar behavior has been suggested in a recent study on  $\text{LiN}(\text{CN})_2$  where an anisotropic behavior was

proposed up to 4 GPa and no polymerization was observed up to 22 GPa.<sup>[20]</sup>

To understand why this happens during the compression from 0 to 13 GPa, we provide COHP plots of the cells (Figure 3c). Again, starting from 0 to 5 GPa, we see only miniscule changes in the COHP plots, resulting in a slightly more covalent system and a reduction of the bandgap from 1.7 to 1.5 eV. This is in line with the pDOS plots shown in Figure 3d. The long Pb–N bonds remain more or less non-bonding, while the shorter bonds show some antibonding contributions below the Fermi level, often observed in metastable compounds.<sup>[3c,21]</sup> Upon looking at the results for 13 GPa, there is a rise of antibonding contributions for all bonds and a significantly broadened DOS. Due to the structural transformation the bandgap opens up to 2.0 eV, without significant changes in the charge distribution. A Mulliken charge analysis of the three models yields charges of +0.99, +0.98, and +0.97 e for Pb at 0, 5, and 13 GPa, respectively. However, the charge distribution within the cyanamide unit is somewhat reduced under pressure (Table 3).

The system lost its two-dimensional character, and the space offered by the weak dispersion interaction between the corrugated double layers gets compressed. To avoid a higher coordination of lead, the cyanamide unit tilts towards the  $a$  axis. This flattening of the double layers results in an unusual elongation of the  $a$  axis between 5 and 9 GPa.

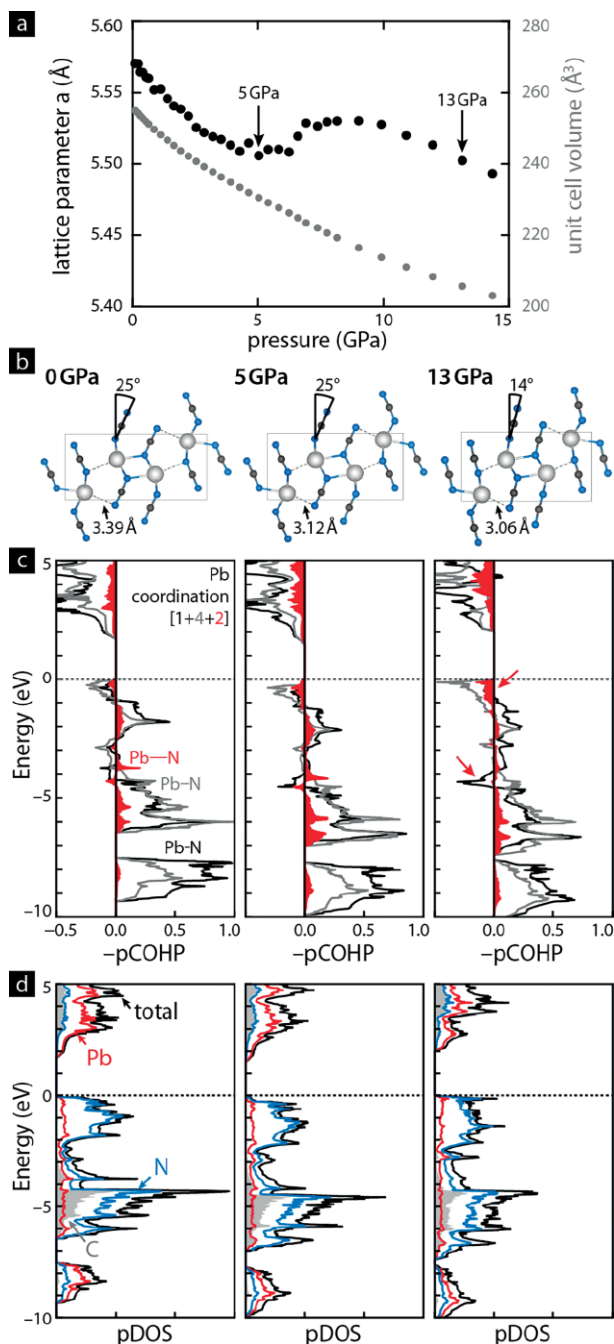


**Figure 3.** (a) Theoretical behavior of the  $a$  lattice parameter and the unit cell volume. (b) Structural variations, (c) pCOHP, and (d) pDOS of PbNCN at 0, 5, and 13 GPa.

**Table 3.** Mulliken charge distribution of PbNCN at 0, 5, and 13 GPa. Charges are given in multiples of  $e$ .

Atom	0 GPa	5 GPa	13 GPa
Pb1	0.99	0.98	0.97
C1	0.28	0.25	0.21
N1	-0.61	-0.60	-0.58
N2	-0.65	-0.63	-0.59

## Conclusions

The high-pressure behavior of lead cyanamide, PbNCN, was studied using the diamond anvil cell technique and in situ X-ray powder diffraction. PbNCN can be characterized as a very soft material, as a zero pressure bulk modulus of  $K_0 = 19(2)$  GPa was measured. In accordance to this, the linear compression moduli of the  $b$  and  $c$  axis were small [ $K_{b0} = 37.7(7)$  GPa and  $K_{c0} = 15.5(2)$  GPa], whereas the linear compression modulus of the  $a$  axis shows a higher value [ $K_{a0} = 145(7)$  GPa]. For a deeper understanding of these results, DFT calculations were employed. The calculations show an unusual behavior of the  $a$  axis, indicating a transition from a typical compression behavior of a two-dimensional layered structure to a more complex one avoiding a sevenfold coordination of  $\text{Pb}^{2+}$  with increasing pressure by tilting the  $\text{NCN}^{2-}$  unit without altering its shape.

The case of PbNCN indicates that metal cyanamides and carbodiimides can have strongly anisotropic compression behavior such that further studies, especially on magnetic transition-metal compounds, have the potential for unexpected phase transitions and non-linear properties.

## Acknowledgements

We acknowledge support by the Deutsche Forschungsgemeinschaft and the Jülich-Aachen Research Alliance (JARA-HPC project jara0033).

**Keywords:** Cyanamide; Lead; DFT calculation

## References

- [1] A. Frank, N. Garo, *Ger. Pat.* **1895**, 88363.
- [2] a) M. G. Down, M. J. Haley, P. Hubberstey, R. J. Pulham, A. E. Thunder, *J. Chem. Soc., Chem. Commun.* **1978**, 52–53; b) K. M. Adams, M. J. Cooper, M. J. Sole, *Acta Crystallogr.* **1964**, *17*, 1449–1451; c) M. Becker, M. Jansen, *Solid State Sci.* **2000**, *2*, 711–715.
- [3] a) U. Berger, W. Schnick, *J. Alloys Compd.* **1994**, *206*, 179–184; b) A. J. Corkett, P. M. Konze, R. Dronskowski, *Z. Anorg. Allg. Chem.* **2017**, *643*, 1456–1461; c) A. Corkett, P. Konze, R. Dronskowski, *Inorganics* **2017**, *6*, 1–10.
- [4] a) X. Liu, P. Müller, P. Kroll, R. Dronskowski, W. Wilmann, R. Conradt, *ChemPhysChem* **2003**, *4*, 789–789; b) X. Liu, P. Müller, P. Kroll, R. Dronskowski, *Inorg. Chem.* **2002**, *41*, 4259–4265; c) R. Riedel, A. Greiner, G. Miehe, W. Dressler, H. Fuess, J. Bill, F. Aldinger, *Angew. Chem. Int. Ed. Engl.* **1997**, *36*, 603–606.
- [5] a) M. Launay, R. Dronskowski, *Z. Naturforsch. B: J. Chem. Sci.* **2005**, *60*, 437–448; b) X. Tang, H. Xiang, X. Liu, M. Speldrich, R. Dronskowski, *Angew. Chem. Int. Ed.* **2010**, *49*, 4738–4742; c) X. Liu, L. Stork, M. Speldrich, H. Lueken, R. Dronskowski, *Chem. Eur. J.* **2009**, *15*, 1558–1561; d) X. Liu, M. Krott, P. Müller, C. Hu, H. Lueken, R. Dronskowski, *Inorg. Chem.* **2005**, *44*, 3001–3003.
- [6] a) O. Reckeweg, F. J. DiSalvo, *Z. Anorg. Allg. Chem.* **2003**, *629*, 177–179; b) M. Neukirch, S. Tragl, H. J. Meyer, *Inorg. Chem.* **2006**, *45*, 8188–8193; c) J. Glaser, L. Unverfehrt, H. Bettentrup, G. Heymann, H. Huppertz, T. Jüstel, H. J. Meyer, *Inorg. Chem.* **2008**, *47*, 10455–10460.

- [7] D. Ressnig, M. Shalom, J. Patscheider, R. More, F. Evangelisti, M. Antonietti, G. R. Patzke, *J. Mater. Chem. A* **2015**, *3*, 5072–5082.
- [8] a) A. Eguia-Barrio, E. Castillo-Martinez, X. Liu, R. Dronskowski, M. Armand, T. Rojo, *J. Mater. Chem. A* **2016**, *4*, 1608–1611; b) M. T. Sougrati, A. Darwiche, X. Liu, A. Mahmoud, R. P. Hermann, S. Jouen, L. Monconduit, R. Dronskowski, L. Stievano, *Angew. Chem. Int. Ed.* **2016**, *55*, 5090–5095.
- [9] H. Liu, W. Klein, H. Bender, M. Jansen, *Z. Anorg. Allg. Chem.* **2002**, *628*, 4–6.
- [10] X. Liu, RWTH Aachen University, Aachen, Germany **2002**.
- [11] A. Dewaele, P. Loubeyre, M. Mezouar, *Phys. Rev. B* **2004**, *70*, 094112.
- [12] J. P. Perdew, K. Burke, M. Ernzerhof, *Phys. Rev. Lett.* **1996**, *77*, 3865–3868.
- [13] a) A. Tkatchenko, R. A. DiStasio, R. Car, M. Scheffler, *Phys. Rev. Lett.* **2012**, *108*, 236402; b) A. Ambrosetti, A. M. Reilly, R. A. DiStasio, A. Tkatchenko, *J. Chem. Phys.* **2014**, *140*, 18A508; c) T. Bučko, S. Lebègue, T. Gould, J. G. Ángyán, *J. Phys.: Condens. Matter* **2016**, *28*, 045201.
- [14] P. E. Blöchl, *Phys. Rev. B* **1994**, *50*, 17953–17979.
- [15] a) G. Kresse, J. Furthmüller, *Phys. Rev. B* **1996**, *54*, 11169–11186; b) G. Kresse, J. Furthmüller, *Comput. Mater. Sci.* **1996**, *6*, 15–50; c) G. Kresse, D. Joubert, *Phys. Rev. B* **1999**, *59*, 1758–1775.
- [16] a) R. Dronskowski, P. E. Blöchl, *J. Phys. Chem.* **1993**, *97*, 8617–8624; b) V. L. Deringer, A. L. Tchougréeff, R. Dronskowski, *J. Phys. Chem. A* **2011**, *115*, 5461–5466; c) S. Maintz, V. L. Deringer, A. L. Tchougréeff, R. Dronskowski, *J. Comput. Chem.* **2013**, *34*, 2557–2567; d) S. Maintz, V. L. Deringer, A. L. Tchougréeff, R. Dronskowski, *J. Comput. Chem.* **2016**, *37*, 1030–1035.
- [17] X. Liu, A. Decker, D. Schmitz, R. Dronskowski, *Z. Anorg. Allg. Chem.* **2000**, *626*, 103–105.
- [18] R. J. Angel, *Rev. Mineral. Geochem.* **2000**, *41*, 35–59.
- [19] M. Becker, M. Jansen, *Z. Anorg. Allg. Chem.* **2000**, *626*, 1639–1641.
- [20] D. W. Keefer, H. Gou, A. P. Purdy, A. Epshteyn, D. Y. Kim, J. V. Badding, T. A. Strobel, *J. Phys. Chem. A* **2016**, *120*, 9370–9377.
- [21] M. Küpers, P. M. Konze, S. Maintz, S. Steinberg, A. M. Mio, O. Cojocaru-Mirédin, M. Zhu, M. Müller, M. Luysberg, J. Mayer, M. Wuttig, R. Dronskowski, *Angew. Chem. Int. Ed.* **2017**, *56*, 10204–10208.

Received: September 2, 2018

Published online: ■

A. Möller, P. M. Konze, R. Dronskowski\* ..... 1–6

High-Pressure Behavior of Lead Cyanamide PbNCN

